

# Impedance Modulation for Negotiating Control Authority in a Haptic Shared Control Paradigm

Vahid Izadi<sup>1</sup>, Akshay Bhardwaj<sup>2</sup>, and Amir H. Ghasemi<sup>3</sup>

**Abstract**—Communication and cooperation among team members can be enhanced significantly with physical interaction. Successful collaboration requires the integration of the individual partners’ intentions into a shared action plan, which may involve a continuous negotiation of intentions and roles. This paper presents an adaptive haptic shared control framework wherein a human driver and an automation system are physically connected through a motorized steering wheel. By the virtue of haptic feedback, the driver and automation system can monitor each other actions, and can still intuitively express their control intentions. The objective of this paper is to develop a systematic model for an automation system that can vary its impedance such that its interaction with a human partner occurs as smoothly as that same interaction would occur between two humans. To this end, we defined a cost function that not only ensures the safety of the collaborative task but also takes account for the assistive behavior of the automation system. We employed a predictive controller based on modified non-negative least square to modulate the automation system impedance such that the cost function is optimized. The results demonstrate the significance of the proposed approach for negotiating the control authority, specifically when human and automation are in a non-cooperative mode. Furthermore, the performance of the adaptive haptic shared control is compared with the traditional haptic shared control paradigm. Finally, future experimental plan, its challenges, and our solution for those challenges are discussed.

## I. INTRODUCTION

Haptic shared control is an emerging research topic with a wide range of applications in the areas such as smart manufacturing, autonomous driving, rehabilitation, health-care, education, and training [1]–[7]. Traditionally, interactive robots were designed to act mainly as a reactive followers where the robot (with some level of autonomy) followed the human’s commands [8]–[10]. However, this type of master-servant arrangement does not capture the sense of partnership [11]–[13] that we mean when we speak of two humans cooperatively moving a piece of furniture. A robot as a pro-active partner should be capable of monitoring human actions, as well as communicating its behavior, and even negotiating and exchanging roles with a human partner [14], [15]. These criteria give rise to a set of fundamental questions that we aim to answer in this research. For instance, (1) what are the interaction models between a human and co-robot in

a Haptic Shared Control framework? (2) Knowing the interaction models, how should a co-robot facilitate exchanging roles dynamically? (3) What strategies should a robot take to create consensus with a human while also guaranteeing the safety and performance of the task? Moreover, (4) how may uncertainty in the behavior of the human-operator affect these interaction models and consensus models?

To seamlessly combine the commands of a human operator and automation system, most of the existing efforts have been devoted to designing an interface so that the human’s high-level commands (human’s intention), can be exploited. Specifically, in the context of physical human-robot interaction, force/torque sensors are embedded in the haptic interface for recognizing human’s intentions and consequently adjusting the robot’s behavior. However, when the automation system and human operator simultaneously interact with each other (especially in an uncertain environment), the force sensors measurements are insufficient for determining the human’s intents. To resolve this issue, we propose to measure the human’s impedance (stiffness of the muscles) as a potential indicator for determining how a human operator dynamically exchange his role (leader/follower) within a collocative task. We argue if the roles of the two agents are agreed upon, then an appropriately timed nudge from one agent can be interpreted by the other and followed or optionally hindered.

To solve an optimal control problem, there are some approaches like LP, QP and LS. The constraints on the control signal or the states play the main role in dynamic solutions. In this paper, to achieve to a non-negative value for the automation’s impedance with a computationally inexpensive method, a modified version of non-negative least squares (MNNLS) is provided.

The outline of this paper is as follow. Sections 2 presents the basics of adaptive haptic shared control paradigm. Section 3 presents the basics of a controller that adaptively modulate the automation’s impedance. Section 4 presents numerical results, and section 5 is the conclusion where we also discussed our future plans.

## II. ADAPTIVE HAPTIC SHARED CONTROL FRAMEWORK

Figure 1 shows a schematic of an adaptive haptic shared control. Three entities each impose a torque on the steering wheel: a human driver through his hands, an automation system through a motor, and the road through the steering linkage. The driver model consists of a cognitive controller, coupled with a biomechanics subsystem. In Figure 1,  $\theta_H$  represent the humans intent, which is an output of the

<sup>1</sup> Vahid Izadi is with Department of Mechanical Engineering, the University of North Carolina at Charlotte, Charlotte, NC, 28223, vizadi@uncc.edu

<sup>2</sup> Akshay Bhardwaj is with Department of Mechanical Engineering, University of Michigan, Ann Arbor, MI, 48109, akshaybh@umich.edu

<sup>3</sup> Amir H. Ghasemi with the Department of Mechanical Engineering, the University of North Carolina at Charlotte, Charlotte, NC, 28223 ah.ghasemi@uncc.edu

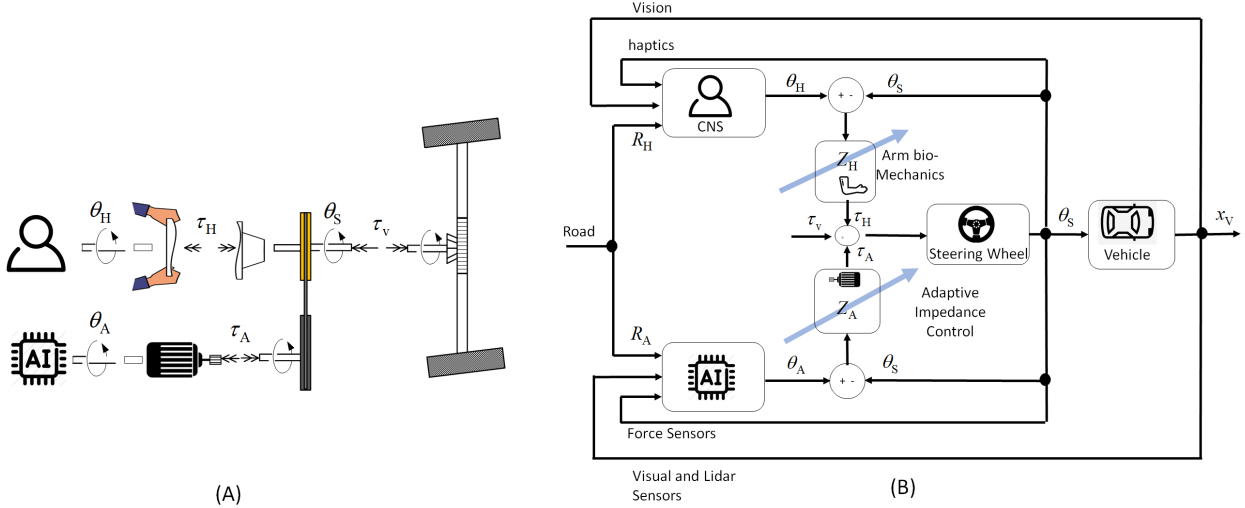


Fig. 1. (A): A general model of control sharing between driver and automation. (B): A block diagram is laid out to highlight the interaction ports between subsystems.

cognitive controller, and impedance  $Z_H$  represent the humans biomechanics. The human biomechanics is backdriveable (the impedance is not infinite), and to indicate that driver impedance varies with changes in grip on the steering wheel, use of one hand or two, muscle co-contraction, or posture changes, we have drawn an arrow through  $Z_H$ . In this paper, the driver and automation system are both shown with a similar structure. Specifically, the automation system is modeled as a higher-level controller (AI) coupled with a lower-level impedance controller. The focus of this paper is on the design of a backdrivable impedance  $Z_A$ . That is, the automation is not designed to behave as an ideal torque source. Rather, the automation imposes its command torque  $\theta_A$  through an impedance  $Z_A$  which can be varied under control of the automation to express the automations current level of control authority. Furthermore, the reference signals  $R_H$  and  $R_A$  represent the goals of the driver and the automation system, respectively. It should be noted that these goals may not be necessarily the same, which is when the negotiation of control authority becomes important. From the model presented in Figure 1, it follows that the position of the steering wheel  $\theta_S$  is a function of the humans intent  $\theta_H$ , automations intent  $\theta_A$ , and the torque applied from the road  $\tau_V$ . Specifically, for a certain impedance, the steering wheel angle is

$$\hat{\theta}_{SW} = \frac{\hat{Z}_H \hat{\theta}_H + \hat{Z}_A(s) \hat{\theta}_A(s) + \hat{\tau}_V(s)}{J_{eq} + B_{SW}s + \hat{Z}_H + \hat{Z}_A} \quad (1)$$

where  $J_{eq} = J_{SW} + J_H + J_A$ ; where  $J_{SW}$  is the steering wheel inertia,  $J_H$  is the inertia of human's hand and  $J_A$  is the inertia of a motor.

It follows from (1) by changing his impedance (increasing  $Z_H$  by co-contracting muscles), the human driver can increase his control authority. Likewise, the automation can be designed such that by imposing higher impedance it requests a higher control authority. In this paper, we define the level of

authority as a relationship between the human's impedance and automation's impedance ( $\frac{Z_H}{Z_A}$ ).

To present how impedance may evolve in time, we introduce the following dynamic models:

$$\dot{Z}_H(t) = \alpha_H Z_H(t) + \beta_H \Gamma_H(t) \quad (2)$$

$$\dot{Z}_A(t) = \alpha_A Z_A(t) + \beta_A \Gamma_A(t) \quad (3)$$

where  $Z_H = [B_H \ K_H]^T$  and  $K_H$  and  $B_H$  are the stiffness and damping associated with humans' biomechanics;  $Z_A = [B_A \ K_A]^T$  and  $K_A$  and  $B_A$  are the stiffness and damping associated with the motor's lower-level proportional-derivative controller;  $\Gamma_H = [\Gamma_{bH}(t) \ \Gamma_{kH}(t)]^T$  is the humans control action for modulating his impedance and  $\Gamma_A = [\Gamma_{bA}(t) \ \Gamma_{kA}(t)]^T$  is the automations control input for modulating its impedance. Additionally,

$$\alpha_H = \begin{bmatrix} \alpha_{bH} & 0 \\ 0 & \alpha_{kH} \end{bmatrix}, \quad \beta_H = \begin{bmatrix} \beta_{bH} & 0 \\ 0 & \beta_{kH} \end{bmatrix} \\ \alpha_A = \begin{bmatrix} \alpha_{bA} & 0 \\ 0 & \alpha_{kA} \end{bmatrix}, \quad \beta_A = \begin{bmatrix} \beta_{bA} & 0 \\ 0 & \beta_{kA} \end{bmatrix} \quad (4)$$

where  $\{\alpha_{bH}, \alpha_{kH}, \alpha_{bA}, \alpha_{kA}, \beta_{bH}, \beta_{kH}, \beta_{bA}, \beta_{kA}\}$  are constant parameters. This formulation captures how impedance evolves in time. Ideally, to determine an optimal behavior for the automation system, optimization should be performed over all control signals of the automation system (i.e.,  $\theta_A, \Gamma_A$ ); However, the focus of this paper is to determine  $\Gamma_A$  as means for allocating the level of authority between the driver and the automation system.

### III. IMPEDANCE MODULATION CONTROLLER DESIGN

In this section, we present a predictive controller for modulating the automation impedance such that the assistive behavior of the automation system improves while the safety of the task is also guaranteed.

First, let the discrete-time model of the impedance dynam-

ics (2) and (3) be

$$Z_H(k+1) = \tilde{\alpha}_H Z_H(k) + \tilde{\beta}_H \Gamma_H(k) \quad (5)$$

$$Z_A(k+1) = \tilde{\alpha}_A Z_A(k) + \tilde{\beta}_A \Gamma_A(k) \quad (6)$$

where  $\tilde{\alpha}_A = I + T_s \alpha_A$ ,  $\tilde{\alpha}_H = I + T_s \alpha_H$ ,  $\tilde{\beta}_A = T_s \beta_A$ , and  $\tilde{\beta}_H = T_s \beta_H$  and  $T_s$  is the sampling time. Furthermore, we define

$$\dot{\theta}_i(k) = \frac{\theta_i(k) - \theta_i(k-1)}{T_s} \quad (7)$$

where  $i = \{\text{SW}, \text{H}, \text{A}\}$ .

Next, let us define a cost function  $J(k)$  in the form of

$$\min_{\Gamma_A} J(k) = \sum_{j=1}^{N_p} \{ \|\tau_H(k+j) + \tau_A(k+j) - \varepsilon(k+j)\| + \|\tau_H(k+j) - \tau_A(k+j)\| \} \quad (8)$$

where  $\tau_H(k) = Z_H[\theta_H(k) - \theta_S(k)]$  and  $\tau_A = Z_A[\theta_A - \theta_S(k)]$ . The first term of the cost function is to ensure safe steering. Specifically, we define  $\varepsilon$  as a minimum required torque that can guarantee the safe maneuver. In this paper, we assume  $\varepsilon$  is known. The second term of the cost function is to minimize the disagreement between a human driver and the automation system. Since the steering angle,  $\theta_S$  and the rate of its changes can be directly measured from the sensor, we simplify the cost function (8) into

$$\min_{\Gamma_A} J(k) = \sum_{j=k+1}^{k+N_p} \{ \|\|Z_H(j)\theta_H(j) + Z_A(j)\theta_A(j) - \varepsilon(j)\| + \|Z_H(j)\theta_H(j) - Z_A(j)\theta_A(j)\| \} \quad (9)$$

In this paper, we assume  $Z_H$  and  $\theta_H$  are known and can be measured. The estimation of human backdrive impedance has a long and rich history in biomechanics and more recent history in the field of haptic rendering. In the context of the adaptive haptic shared control paradigm, parallel with this work, authors are focused on developing a method to obtain a continually-updated estimate of the backdrive impedance of the human driver. With access to an online estimate of the driver's time-varying impedance, as well as the torque on the steering wheel (using a differential torque) sensor, we can estimate the human's intent  $\theta_H$ . In this paper, we assume the  $Z_H$  and  $\theta_H$  is given and known.

The goal in the cost function is to determine  $\Gamma_A$  such that the cost function  $J$  is minimized. To this end, we  $Z_A \theta_A$  can be presented as

$$Z_A \theta_A(k) = B_A(k) \left[ \frac{\theta_A(k) - \theta_A(k-1)}{T_s} \right] + K_A(k) \theta_A(k) \quad (10)$$

By replacing  $B_A$  and  $K_A$  from Eq. xx, we will have:

$$Z_A \theta_A(k) = \{\Phi(k) + \Psi(k)\} \begin{bmatrix} \theta_A(k) \\ \theta_A(k-1) \end{bmatrix} \quad (11)$$

$$\Phi(k) = \tilde{\alpha}_A \left[ \frac{B_A(k-1)}{T_s} + K_A(k-1) \quad -\frac{B_A(k-1)}{T_s} \right] \quad (12)$$

$$\Psi(k) = \tilde{\beta}_A \left[ \frac{\Gamma_{BA}(k)}{T_s} + \Gamma_{KA}(k) \quad -\frac{\Gamma_{BA}(k)}{T_s} \right] \quad (13)$$

The  $\Phi$  and  $\Psi$  represents intrinsic mechanical impedance and control action vectors, respectively. By propagating the automation torque for the next time steps until  $N_p$  step, the  $\Phi$  and  $\Psi$  vectors will move forward in the time. In order to create prediction matrices we can rearrange the  $N_p$  step automation torque vector like following equation:

$$Z_A \Theta_A = \bar{\Theta} \Omega(\Phi, \Psi) \quad (14)$$

where

$$Z_A \Theta_A = \begin{bmatrix} Z_A(k+N_p)\theta_A(k+N_p) \\ \vdots \\ Z_A(k+1)\theta_A(k+1) \\ Z_A(k)\theta_A(k) \end{bmatrix} \quad (15)$$

$$\bar{\Theta}^T = \begin{bmatrix} \theta_A(k+N_p) & \cdots & 0 & 0 \\ \theta_A(k+N_p-1) & \cdots & 0 & 0 \\ \vdots & \ddots & \vdots & \vdots \\ 0 & \cdots & \theta_A(k+1) & 0 \\ 0 & \cdots & \theta_A(k) & 0 \\ 0 & \cdots & 0 & \theta_A(k) \\ 0 & \cdots & 0 & \theta_A(k-1) \end{bmatrix} \quad (16)$$

$\Omega(\Phi, \Psi)$

$$= \begin{bmatrix} \{(\tilde{\alpha}_A)^{N_p}[\Delta(k)] + (\tilde{\alpha}_A)^{N_p-1}\Psi(k+1) + \dots + \Psi(k+N_p)\}^T \\ \vdots \\ \{\tilde{\alpha}_A[\Delta(k)] + \Psi(k+1)\}^T \\ \{\Delta(k)\}^T \end{bmatrix} \quad (17)$$

where  $\Delta(k) = \Phi(k) + \Psi(k)$ .

According to the second term of (9), in the ideal model, the value of  $Z_H \theta_H$  will be equal to  $Z_A \theta_A$ . On the other hand, in the (15), the amount of automation control action at time step  $k$  can be determined by using the methods like linear programming (LP), quadratic programming (QP) and least square (LS). As it can be seen in the (15), the solution from the optimal solver will give us the summation of  $\Phi$  and  $\Psi$ . In the LP, QP, and LS method, it is possible to have a negative value. This means, the mechanical link on the automation side is disconnected (has zero impedance). In this paper, instead of these methods, the Non-Negative LS method is used, which guaranteed to solve the cost function with a non-negative solution. Furthermore, we used a modified version of NNLS to solve the cost function and reduce the computational burden. In the following section,

the MNNLS method is presented.

#### A. Modified Non-Negative Least Squares Method

Since the impedance is a non-negative parameter, to solve cost function (9), the conventional Linear Square algorithm must be rearranged. A non-negative LS is an LS optimization problem which is subjected to non-negativity constraints. A simple, approximate way to implement these constraints is to solve the corresponding unconstrained LS problem and then overwrite any negative values with zeros. However, a challenge associated with overwriting negative values in LS method is that it may not result in converging to a minimum possible error on successive iterations. To resolve this limitation, there are several mathematically proven methods to solve Non-Negative LS problems [16]–[18], which impose non-negativity criteria on the solution while minimizing the sum of squared residuals between the data being fitted and their estimates in a true LS sense.

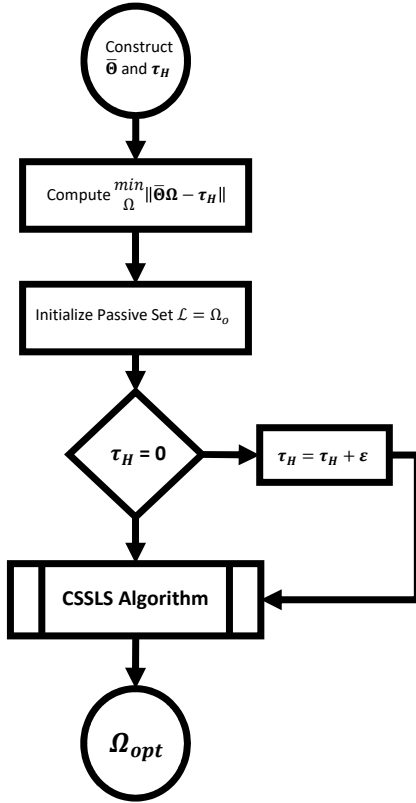


Fig. 2. MNNLS algorithm

The performance of the NNLS in the large-scale problems which we have large horizon estimation is the main consideration in controller design. Pre-computing the cross product and pseudo-inverses (inverse) matrices are the essential tools for improving the NNLS performance. To resolve this challenge, in this paper, we used a modified NNLS by the following flowchart [17]. The compensatory term in the NNLS is considered in the case of zero impedance from the driver which means the measurement vector is the summation of the human’s torque and predefined  $\epsilon$  value.

## IV. NUMERICAL RESULTS

In this section, we present a series of numerical results to show the effectiveness of the proposed adaptive haptic shared control (HSC) for improving the collaboration between the human driver and automation system. We specifically consider two modes of interactions: cooperative and non-cooperative. A cooperative mode is when  $R_H$  and  $R_A$  (see Fig. 1) have the same sign and non-cooperative mode is when the sign of  $R_H$  and  $R_A$  is different. In this paper, we assume  $\theta_H$  and  $\theta_A$  which are the outputs of a higher-level controller (e.g., MPC-based controller) are known and given. We aim to determine an optimal  $\Gamma_A$  such that the cost function  $J$  defined in (9) is minimized. For all the simulation results presented below, the steering wheel inertia is  $J_{SW} = 0.1$  (N.m/s<sup>2</sup>) and damping coefficient for the steering wheel is  $B_{SW} = 0.01$  (N.m/s). Also, the human’s hand inertia is  $J_H = 0.001$ (N.m/s<sup>2</sup>) [19] and the motor inertia is  $J_A = J_H$ . The sampling time is  $T_s = 0.1$  second and the control and estimation horizon is  $N_p = 20$ .

Figure 3 demonstrates a cooperative mode of interaction between a human driver and an automation system when both driver and automation intentions have the same sign ( $\text{sgn}(\theta_H) = \text{sgn}(\theta_A)$ ). The human’s impedance is shown with red dashed lines. We consider a scenario wherein the human’s impedance is adaptively changing thought time. Specifically,  $K_H$  initial value is 1 N.rad and at  $t = 8$  and  $t = 20$  seconds, it changes from 1 N.rad to 0.05 N.rad and from 0.05 N.rad to 0.75 N.rad, respectively. Figure 3-c shows that automation tries to match its impedance with the human driver in a cooperative task.

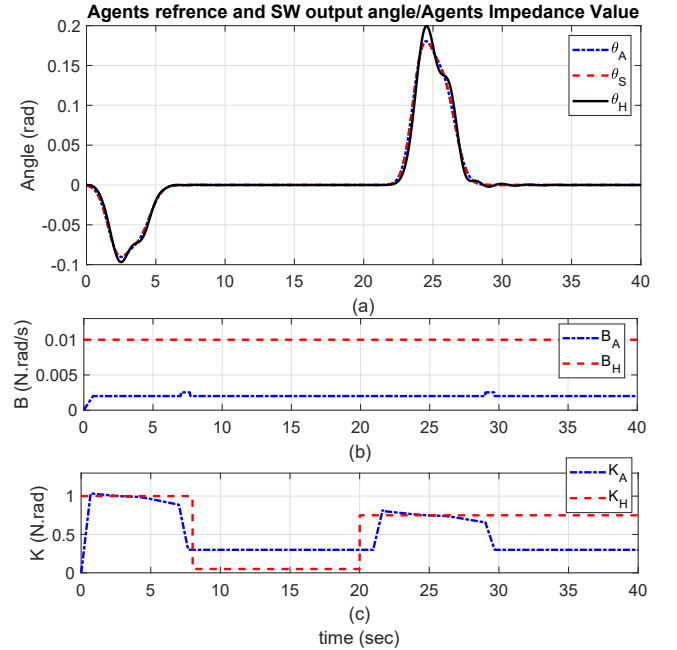


Fig. 3. Cooperative mode of integration between a human driver and an automation system with adaptive HSC

Figure 4 demonstrate a non-cooperative mode of integration between a human driver and an automation system

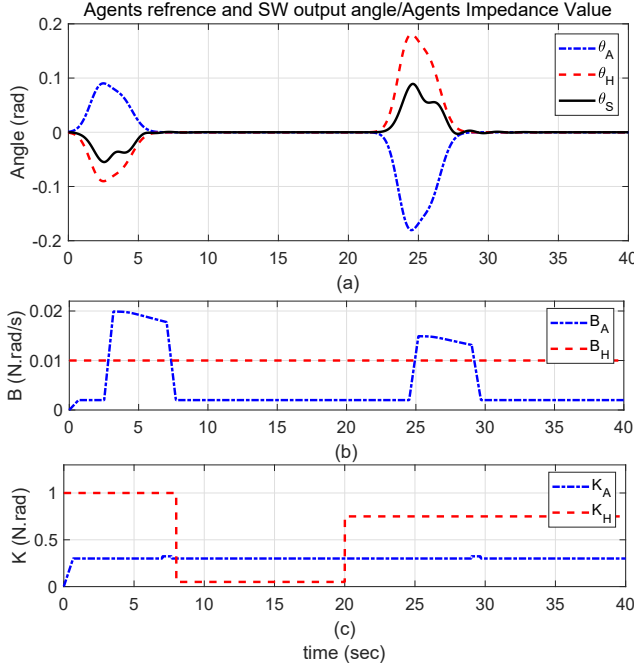


Fig. 4. Non-cooperative mode of integration between a human driver and an automation system with adaptive HSC

when the driver and automation intentions have different signs ( $\text{sgn}(\theta_H) \neq \text{sgn}(\theta_A)$ ). Similar to Figure 3, the human's impedance dynamically changes with time. However, to reduce the disagreement between the two agents, the automation system adopts a smaller impedance. It should be noted that during  $0 < t < 20$  when the human's impedance is low and not sufficient for safely maneuvering the steering wheel (i.e.,  $|\tau_H| < \varepsilon$ ), then the automation system adopt a higher impedance to ensure the safe maneuver.

Figure 5 shows how different values of  $\varepsilon$  may affect the steering angle as well as the differential torque (fight between the two agents) in the non-cooperative mode. By selecting higher values for the minimum torque required for the safe maneuver  $\varepsilon$ , the differential torque becomes bigger, and human's and automation's input will cancel each other (lower values of  $\theta_S$ ).

Next, we compare the performance of a non-adaptive (when the automation impedance does not change as the human's impedance changes) and adaptive haptic shared control paradigms. Figure 6 demonstrates the driver and automation interaction within a non-cooperative interaction mode. Considering  $\varepsilon = .1$ , the right-hand side plots present the impedance and steering angle with impedance modulation (adaptive), while the left-hand shows them without impedance modulation (non-adaptive). It follows from Fig 6 that in non-adaptive mode, the driver's and automation's control command cancel out and the steering wheel is almost zero ( $\theta_S \approx 0$ ). However, this issue has been solved in the adaptive haptic shared control. Additionally, the disagreement between two agents in the adaptive haptic shared control paradigm is much lower than the non-adaptive haptic mode.

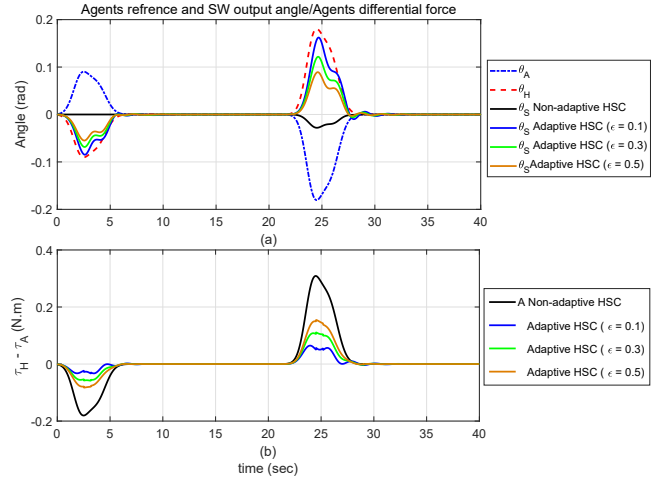


Fig. 5. (a) The effect of the different values of  $\varepsilon$  on the steering wheel angle and (b) its effect on the differential torque between human and automation

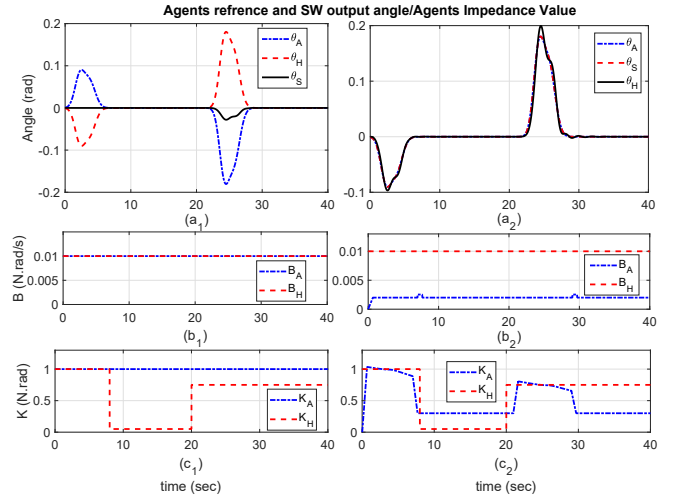


Fig. 6. Comparison between adaptive and non-adaptive haptic shared control paradigms

## V. CONCLUSIONS AND FUTURE PLANS

This paper presents the principles of adaptive haptic shared control paradigm. Specifically, we introduce the impedance modulation as one possible mechanism for negotiation of the control authority. We propose a predictive control approach where the impedance of an automation system is modulated so that the fight between the two agents is minimized while the safety of the system is guaranteed. In the future, we plan to extend the outcomes of this research to experimental studies. To this end, we have developed a low-fidelity fixed-base driving simulator (see Fig. 7). The simulator features a steering wheel that is motorized, and a screen that displays a virtual driving environment. The steering wheel is further equipped with a force sensor that is within easy reach of driver's hands.

In this paper, we have assumed that driver intent  $\theta_H$  and driver impedance  $Z_H$  are available. However, in an actual driving experiment we would need to estimate these



parameters online. In the past, it has been shown that the grip force can be used as a proxy to estimate the driver impedance [20], [21]. Accordingly, in our driving experiments in the future, we plan to use the grip force sensor measurements to estimate the human's impedance on the fly. Additionally, to have an approximate estimate the human's intent  $\theta_H$ , we plan to ask the participants to follow a pre-designed path. By integrating this online information about the human's intention (known from a pre-designed path), human's estimated impedance (known from the force sensor), and the automation's intentions (AI's output), we intend to test the performance of the adaptive haptic shared control paradigm proposed in this paper.

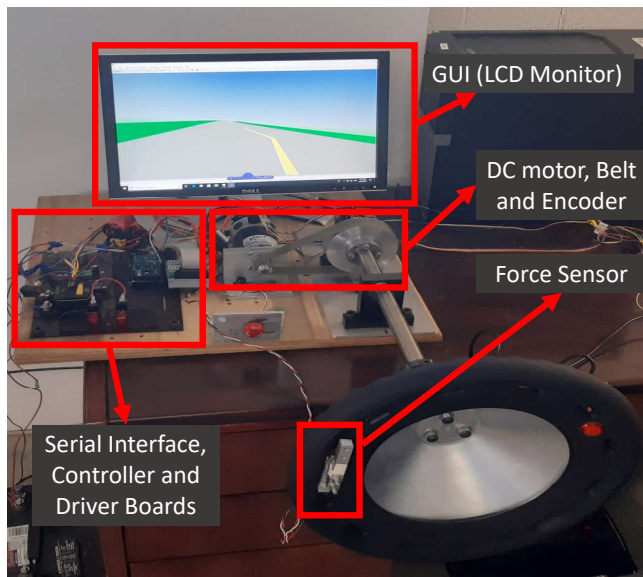


Fig. 7. Fixed base driving simulator: experimental setup.

## REFERENCES

- [1] Arvin Agah. Human interactions with intelligent systems: research taxonomy. *Computers & Electrical Engineering*, 27(1):71–107, 2000.
- [2] A Albu-Schaffer, Antonio Bicchi, G Boccadamo, R Chatila, A De Luca, A De Santis, G Giralt, G Hirzinger, V Lippiello, R Mattone, et al. Physical human-robot interaction in anthropic domains: safety and dependability. In *Proceeding 4th IARP/IEEE-EURON Workshop on Technical Challenges for Dependable Robots in Human Environments*, 2005.
- [3] Pieter Beyl, K Knaepen, S Duerinck, Michaël Van Damme, Bram Vanderborght, R Meeusen, and Dirk Lefeber. Safe and compliant guidance by a powered knee exoskeleton for robot-assisted rehabilitation of gait. *Advanced Robotics*, 25(5):513–535, 2011.
- [4] Amirmahdi Ghasemi, R Nikbakhti, Amirreza Ghasemi, Faraz Hedayati, and Amir Malvandi. Parallelized numerical modeling of the interaction of a solid object with immiscible incompressible two-phase fluid flow. *Engineering Computations*, 34(3):709–724, 2017.
- [5] Amirreza Ghesemi, Jimmy Fox, and Admin Husic. Predicting macroturbulence energy and timescales for flow over a gravel bed: Experimental results and scaling laws. *Geomorphology*, 332:122–137, 2019.
- [6] Nicola Vitiello, Tommaso Lenzi, Stefano Roccella, Stefano Marco Maria De Rossi, Emanuele Cattin, Francesco Giovacchini, Fabrizio Vecchi, and Maria Chiara Carrozza. Neuroexos: A powered elbow exoskeleton for physical rehabilitation. *IEEE Transactions on Robotics*, 29(1):220–235, 2013.
- [7] Akshay Bhardwaj, Amir H Ghasemi, Yingshi Zheng, Huckleberry Febbo, Paramsothy Jayakumar, Tulga Ersal, Jeffrey L Stein, and R Brent Gillespie. Whos the boss? arbitrating control authority between a human driver and automation system. *Transportation Research Part F: Traffic Psychology and Behaviour*, 68:144–160, 2020.
- [8] R Brent Gillespie, M OModhrain, Philip Tang, David Zaretzky, and Cuong Pham. The virtual teacher. In *Proceedings of the ASME Dynamic Systems and Control Division*, volume 64, pages 171–178. American Society of Mechanical Engineers, 1998.
- [9] Douglas P Haanpaa and Gerald P Boston. An advanced haptic system for improving man-machine interfaces. *Computers & Graphics*, 21(4):443–449, 1997.
- [10] Shinsuk Park, Robert D Howe, and David F Torchiana. Virtual fixtures for robotic cardiac surgery. In *International Conference on Medical Image Computing and Computer-Assisted Intervention*, pages 1419–1420. Springer, 2001.
- [11] Ryojun Ikeura, Tomoki Moriguchi, and Kazuki Mizutani. Optimal variable impedance control for a robot and its application to lifting an object with a human. In *Proceedings. 11th IEEE International Workshop on Robot and Human Interactive Communication*, pages 500–505. IEEE, 2002.
- [12] Ryojun Ikeura, Akishi Morita, and Kazuki Mizutani. Variable damping characteristics in carrying an object by two humans. In *Proceedings 6th IEEE International Workshop on Robot and Human Communication. RO-MAN'97 SENDAI*, pages 130–134. IEEE, 1997.
- [13] Hirohiko Arai, Tomohito Takubo, Yasuo Hayashibara, and Kazuo Tanie. Human-robot cooperative manipulation using a virtual nonholonomic constraint. In *Proceedings 2000 ICRA. Millennium Conference. IEEE International Conference on Robotics and Automation. Symposia Proceedings (Cat. No. 00CH37065)*, volume 4, pages 4063–4069. IEEE, 2000.
- [14] Kyle B Reed and Michael A Peshkin. Physical collaboration of human-human and human-robot teams. *IEEE Transactions on Haptics*, 1(2):108–120, 2008.
- [15] Raphaela Groten, Daniela Feth, Harriet Goshy, Angelika Peer, David A Kenny, and Martin Buss. Experimental analysis of dominance in haptic collaboration. In *Robot and Human Interactive Communication, 2009. RO-MAN 2009. The 18th IEEE International Symposium on*, pages 723–729. IEEE, 2009.
- [16] Rasmus Bro and Sijmen De Jong. A fast non-negativity-constrained least squares algorithm. *Journal of Chemometrics: A Journal of the Chemometrics Society*, 11(5):393–401, 1997.
- [17] Mark H Van Benthem and Michael R Keenan. Fast algorithm for the solution of large-scale non-negativity-constrained least squares problems. *Journal of Chemometrics: A Journal of the Chemometrics Society*, 18(10):441–450, 2004.
- [18] Jingu Kim, Yunlong He, and Haesun Park. Algorithms for nonnegative matrix and tensor factorizations: A unified view based on block coordinate descent framework. *Journal of Global Optimization*, 58(2):285–319, 2014.
- [19] Bo Yu, R Brent Gillespie, James S Freudenberg, and Jeffrey A Cook. Human control strategies in pursuit tracking with a disturbance input. In *Decision and Control (CDC), 2014 IEEE 53rd Annual Conference on*, pages 3795–3800. IEEE, 2014.
- [20] Bo Yu, R Brent Gillespie, James S Freudenberg, and Jeffrey A Cook. Identification of human feedforward control in grasp and twist tasks. In *American Control Conference (ACC), 2014*, pages 2833–2838. IEEE, 2014.
- [21] Jeremy D Brown, Andrew Paek, Mashaal Syed, Marcia K OMalley, Patricia A Shewokis, Jose L Contreras-Vidal, Alicia J Davis, and R Brent Gillespie. An exploration of grip force regulation with a low-impedance myoelectric prosthesis featuring referred haptic feedback. *Journal of neuroengineering and rehabilitation*, 12(1):104, 2015.